Energy Dependent Pulse Arrival Times of Accreting Millisecond X-ray Pulsar: MAXI J0911-655

Fang-Ming Gu, Yi Chou, Hung-En Hsieh, Yi-Hao Su
Graduate Institute of Astronomy, Nation Central University, Taiwan

Abstract

MAXI J0911-655 (Swift J0911.9-6452), the 18th known accreting millisecond X-ray pulsar (AMXP) located in globular cluster NGC 2808, was discovered in 2016 with a pulsation period of 2.94 ms. The follow-up observations were made by XMM-Newton and NuSTAR. In this study, we attempted to detect the energy dependent pulse arrival time lags, which have been seen in other AMXPs. To obtain the pulse profile, precise orbital and spin parameters are essential. We first applied the orbital and spin parameters that yielded by previous study and then refined them using pulse arrival time delay technique for the 0.3 to 10 keV events collected by XMM-Newton. These photons were further divided into 10 energy bands and then folded with the best spin and orbital parameters to make the pulse profiles for these bands. The pulse arrival time lags respected to the softest energy band were evaluated through cross correlation of the best fitted pulse profiles. We found the lags can be up to 0.13 cycle (~378 μs) in the energy range of 0.3 to 10 keV. The analyzing of NuSTAR data, whose photon energy may reach to harder energy band (up to ~79 keV), is still processing.

Introduction

Accreting millisecond X-ray pulsars (AMXPs) are a kind of low mass X-ray binary (LMXB) with detectable pulsations of frequency more than a hundred hertz. They are considered as the progenitors of millisecond pulsars in radio band. To date, 20 LMXBs have been verified as AMXPs followed by the first discovered one, SAX J1808.4-3658, in 1998 (Wijnands & van der Klis 1998). All of AXMPs are transient sources.

The 18th identified AXMP, MAXI J0911-655 (also named Swift J0911.9-645), was first detected by MAXI (Serino et al. 2016) on 19th February 2016 in globular cluster NCG2808 during its outburst and the follow-up observations were made with a number of X-ray telescopes, including, Swift, INTEGER, Chandra, XMM-Newton and NuSTAR. Sanna. et .al (2017) (hereafter S17) reported discovery of its pulsations with a period of 2.9 ms form XMM-Newton and NuSTAR observations. Some of orbital parameters, such as orbital period (44.3 min) and a projected semi-major axis (17.6 lt-ms), were immediately resolved using the pulse arrival time delay technique.

Soft lag phenomenon that the pulsation of soft X-ray band lags by one of hard X-ray band by tens to hundreds μs was first report by Cui et. al (1998) for SAX J1808.4-3658 and can be seen in many of AXMPs. For some sources, the lags decrease for even harder X-ray band (called hard lag) that were found in later observations. Cui et. al (1998) proposed that the soft lag is caused by that the soft photons are made by the downscattering of hard photon on the cooler edge of hot spot. On the other hand, Poutanen et .al (2003) suggested a two-component model that the soft lag is made by the different angular distributions between emissions of soft and hard X-ray photons plus Doppler boosting effect. Furthermore, Falanga et .al (2007) a Comptonization model to explain both soft and hard lags.

In this work, we attempt to study the soft/hard lags phenomenon in this newly discovered AMXP, MAXI J0911-655, using the data from XMM-Newton and NuSTAR observations. By combination of the data from these two telescopes, we are able to see this phenomenon in a large X-ray energy range (from 0.3 keV up to 79 keV). Here, we report our preliminary results from XMM-Newton observations. The data analysis of NuSTAR data is processing.

Observation

We analyzed the MAXI J0911-655 data from XMM-Newton observations made on 24 April 2016 (Obs. ID. 0790181401, hereafter xmm401) and on 22 May 2016 (Obs. ID. 0790181501, hereafter xmm501). Both of the observations were used the PN camera in timing mode (with time resolution 30μs), and the exposure times are about 28ks and 35ks. We applied the Science Analysis Software (SAS) v. 16.1.0 with the initial calibration and converted all event arrival times from the local satellite to the barycenter of solar system by BARYCEN. Following S17, we chose the energy range in 0.3 to 10 keV, and extracted the source events round the location of the source.

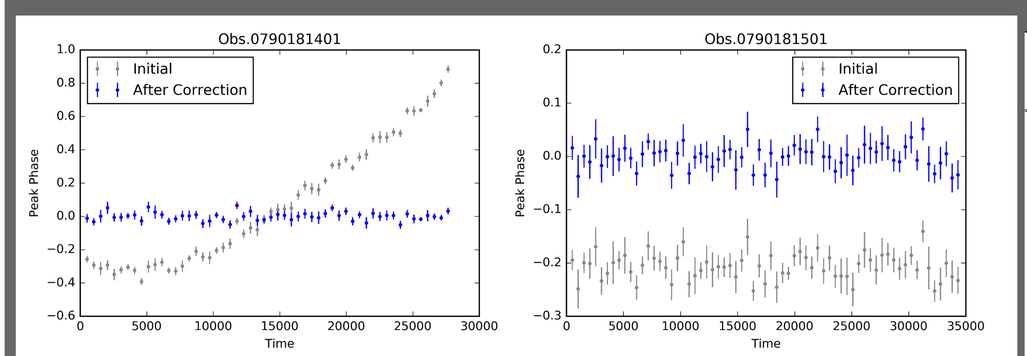

Fig. 1. The pulse phase evolutions for xmm401 (left) and xmm501 (right) using the initial parameters (black) and the ones after corrections (blue).

Table 1. The parameters comparison between S17 and our work.

	Obs. 0790181401		Obs. 0790181501	
	S17	Correction	S17	Correction
ν_{spin} (Hz)	339.975071(3)	339.975119(10)	339.9750123(3)	339.9750125(3)
T_0 (MJD)	0.2 [a]	0.2248736712(7) [a]	0.6 [b]	0.5962765020(3) [b]
A (s)	0.01759(2)	0.01759(2)	0.017598(11)	0.017596(12)
P_{orb} (s)	2659.71(14)	2659.66(5)	2659.93(7)	2659.98(8)
$T_{\pi/2}$ (MJD)	57502.192879(5)	57502.192908(4)	57530.608602(13)	57530.608611(6)
$\dot{\nu}$ (Hz/s)	$-2.76(16)\times10^{-9}$	$-1.63(28)\times10^{-8}$	-	-
$\ddot{\nu}$ (Hz/s^2)	-	$1.83(45)\times10^{-12}$	-	-
$\dddot{\nu}$ (Hz/s^3)	-	$-1.10(32)\times10^{-16}$	-	-

a :days after MJD 57502 、 b: days after MJD 57530

Data Analysis and Result

In order to study the energy-dependence pulse arrival times, we must use the accurate spin and orbital parameters to get precise pulse profile. Although S17 have derived the spin and orbital parameters (listed in Table 1), we still process the similar procedure to confirm and refine them. First, we divided the 0.3-10 keV data of two observations into a number of 512-s segments. Because of the orbital Doppler Effect, the observed pulsar frequency would depend on the orbital phase. We used the Keplerian model and assumed that the binary orbit is circular and the spin frequency of neutron star is constant:

$$\nu(t) = \nu_0 + 2\pi f_{orb}\nu_0 \frac{a\,sin\,i}{c} sin\left[2\pi f_{orb}(t - T_{\pi/2})\right] \quad (1)$$

where ν_0, f_{orb}, $a\ sin\ i$ and $T_{\pi/2}$ are pulsar frequency, orbit frequency, projected of orbital radius and the epoch of 90° mean longitude, respectively. Integrating the equation from phase zero epoch of pulsar T_0 (we tentatively assume T_0 as the first photon arrival time) to the event time t, we could get the cycle count number $N_c(t)$. The phase ϕ is defined as decimal part of cycle count number.

$$\phi = frac(N_c(t)) = frac\left(\int_{T_0}^{t} \nu(t)\,dt\right)$$
$$= frac\left(\nu_0(t - T_0) + \nu_0 \frac{a\sin i}{c}\cos\left[2\pi f_{orb}(t - T_{\pi/2})\right]\right. \quad (2)$$
$$\left. + \nu_0 \frac{a\sin i}{c}\sin\left[2\pi f_{orb}(T_0 - T_{\pi/2})\right]\right)$$

From Eq 2, we may obtain the phase of each event and then folded each 512-s data segment into 20 phase bins to get the pulse profile. We found that not all pulse profiles can be well described as a single sinusoidal function as S17 suggested, which is the reason to re-estimate the orbital and spin parameters. Each pulse profile was modelled as a multiple sinusoidal function and its peak was selected as fiducial point of the pulse. If the parameters are accurate, all the pulse phases will well fitted to a horizontal line at phase zero. However, if there are slightly deviations from the true parameters, the pulse phases will change over time described as a first order approximation equation as Eq. 3 (where A is $a\ sin\ i\ /c$).

$$N_c^0 - N_c = \frac{\partial N_c}{\partial \nu_0}\delta\nu_0 + \frac{\partial N_c}{\partial T_0}\delta T_0 + \frac{\partial N_c}{\partial A}\delta A + \frac{\partial N_c}{\partial f_{orb}}\delta f_{orb} + \frac{\partial N_c}{\partial T_{\pi/2}}\delta T_{\pi/2} + \frac{\partial N_c}{\partial \dot{\nu}}\delta\dot{\nu} + \frac{\partial N_c}{\partial \ddot{\nu}}\delta\ddot{\nu} + \frac{\partial N_c}{\partial \dddot{\nu}}\delta\dddot{\nu} + \cdots \quad (3)$$

We first chose the parameters proposed by SP17 and fitted the detected pulse phase evolution with Eq. 3 to obtain the corrections of parameters. The process described above can be iterated until the corrections of all parameters are less than an order of the corresponding errors. For xmm401 data, we needed to further adding spin frequency derivative terms ($1/2\,\dot{\nu}(t - T_0)^2$, $1/6\,\ddot{\nu}(t - T_0)^3$ and $1/24\,\dddot{\nu}(t - T_0)^4$) to obtain the satisfactory fitting. However, these additional terms are believed due to instrument issue (SP17). Fig. 1. shows the pulse phase evolutions obtained by the initial parameters and refined parameters. The refined orbital and spin parameters are listed in Table 1.

With precise orbital and spin parameters, energy-resolved pulse profiles can be made. We divided these 0.3-10 keV events into 10 energy bands where the numbers of events of these bands are about equal to each other and folded each of them with the refined orbital and spin parameters. We then applied the multiple sinusoidal functions to fit the pulse profiles and used cross-correlation technique to obtain the phase lags relative to the softest energy band.

Fig. 3. show the relative energy-dependent pulse arrival times of two XMM-Newton data sets and the combined data. Significant lag of ~0.13 cycle (~378 μs) between softest band (0.3-0.731 keV) and hardest band (4.685-10.0 keV) can be seen.

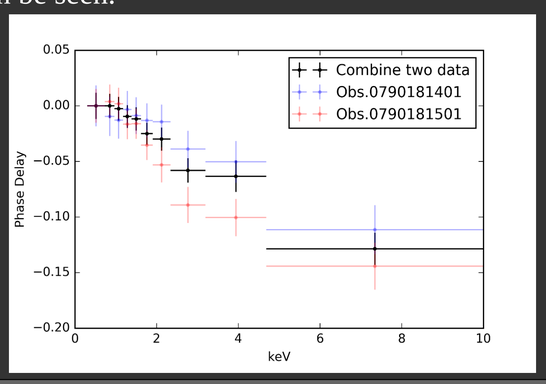

Fig. 3. The energy dependent the pulse arrival time.

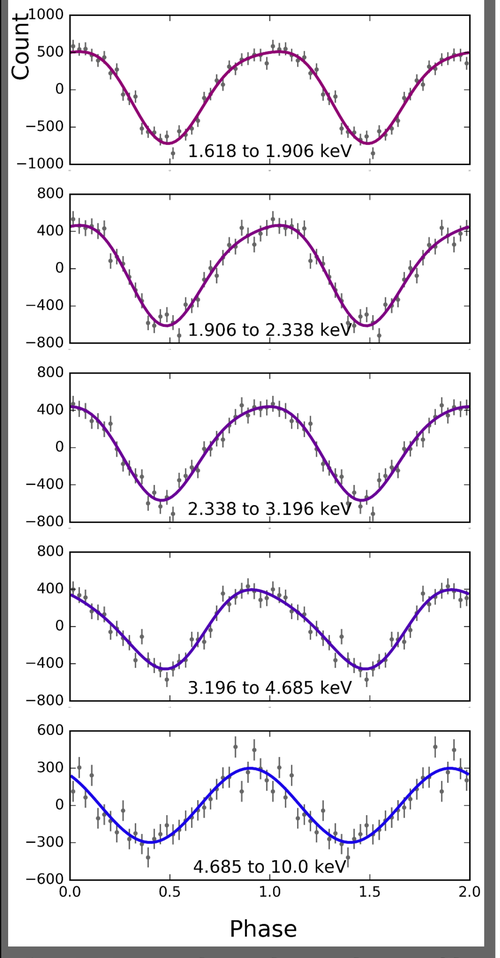

Fig. 2. Energy dependent pulse profile.

Summary and Future Work

In this work, we found the soft lag up to 0.13 cycle (~378 μs) in the MAXI J0911-655, although the lags are slightly different in two observations. In future, we are going to analysis the NuSTAR data to check the energy-dependent phase lags for even higher energy bands in MAXI J0911-655.

Graduate Institute of Astronomy, NCU
國立中央大學天文研究所

Reference

Cui W., Morgan E. H., Titarchuk L. G., 1998, ApJ, 504, L27
Falanga M., Titarchuk L., et .al 2007, ApJ, 661 1084
Poutanen J., & Gierliński M., 2003, MNRAS, 343, 1301
Sanna A., Papitto A., Burderi, L., et al., 2017, A&A, 598, A34
Serino, M., Tanaka, K., Negoro, H., et al. 2016, ATel, 8872, 1
Wijnands, R., & van der Klis, M. 1998, Nature, 394, 344